UNCLASSIFIED



ATOMIC ENERGY

RESEARCH ESTABLISHMENT

# PROTON DYNAMICS IN THE LINEAR ACCELERATOR I. GRID-FOCUSSED SECTION

AN A. E. R. E. REPORT

by

N.M. KING

DEPARTMENT OF ATOMIC ENERGY,
HARWELL, BERKS.
1954

UNCLASSIFIED

# PROTON DYNAMICS IN THE LINEAR ACCELERATOR.
## I. GRID-FOCUSSED SECTION.

by

N. M. King

A B S T R A C T

By assuming a simple form for the fields in the accelerator, equations of motion for the phase and radial oscillations of the protons are derived, susceptible to a gap-by-gap computation. The various approximations involved in the treatment are discussed.

The results of the orbit computations have been interpreted so as to lead to displacement-divergence "phase diagrams" representing the types of beam capable of being focussed in the accelerator, and the resulting beams at 10 MeV have been determined.

The results indicate that, due to large radial excursions of non-synchronous protons, the actual range of particles trapped in phase will be more curtailed than was suggested by previous considerations.

A.E.R.E.,
Harwell, Berks.
April, 1954.

HD.1183

## CONTENTS



## ERRATA

| | | | |
|---|---|---|---|
| SECTION 5 | (i) | line 3 ..... | cut grid<u>s</u> |
| | (ii) | line 5 ..... | b<u>e</u> the "delta |
| | (iii) | line 4 ..... | small importan<u>ce</u> |

## 1. INTRODUCTION

Accurate calculation of the motion of protons in a linear accelerator cannot be achieved until the actual fields present in the machine are known. However, by assuming some simple reasonable form for the fields, we can gain a clear picture of the main aspects of the dynamics of focussing. The chief errors to be expected in such a theory will be due to effects taking place in the first few gaps, where the drift-tubes are not widely separated and the proton velocity is still small. Further investigation of these effects is contemplated.

The machine is designed so that there is a "synchronous" proton which reaches the centre of each gap at a stable phase position, $\varphi_s$, of the radio-frequency axial electric field. This defines the time taken between the centres of successive gaps and the velocity of the proton in successive drift-tubes. The stable phase position has been chosen as $30^\circ$ in front of a peak of the r-f field, and the gaps are taken to be one quarter of the lengths between adjacent drift-tube centres.

Protons injected at times different from that at which the synchronous particle enters the accelerator will oscillate in phase about the stable value, with an adiabatically decreasing amplitude, and in addition, will describe coupled radial oscillations of slowly growing amplitude.

These orbits have been computed for different initial injection phases, and have been interpreted so as to determine the kind of beam which can be focussed in the 10 MeV section, and to give some indication of the beam which will be available at 10 MeV, for injection into the first strong-focussing section.



## 2. FIELDS

The motion of protons in the accelerator will be influencedby both radial and axial forces. The axial forces are due to the longtitudinal component of electric field, $E_z$, whilst the radial forces result from the action of a transverse component of electric field, $E_r$, and the azimuthal radio-frequency magnetic field, $H_\theta$. The latter field is of order $\beta$ times the electric field $E_z$, where $\beta = v/c$, and can be safely ignored.

We shall make the approximation that the field $E_z$ within a gap is uniform except at the entrance; the grids inserted at the beginning of each drift-tube ensure that the axial field is uniform at the end of a gap. In practice, $E_z$ will have some radial variation which will be neglected here.

Thus, we can express the electric field acting on protons within a gap as

$$E_z = E_0 \cos(\omega t - \varphi)$$

where $\omega = 2\pi c/\lambda$, $\lambda$ being the free-space wavelength.

Replacing time t, by $\int v^{-1} . dz$, and writing $k = \omega/v = 2\pi/\beta\lambda$, we obtain

$$E_z = E_0 \cos(\int k \, dz - \varphi) \qquad \ldots\ldots (1)$$

Making use of the divergence relation, $\nabla . \underset{\sim}{E} = 0$, we obtain an expression for the radial electric field.

$$E_r = -\tfrac{1}{2} . r . \frac{dE_z}{dz} \qquad \ldots\ldots (2)$$

3. EQUATIONS OF MOTION.

We shall consider a proton which enters the $n^{th}$ gap of the accelerator with a velocity $v_{n-1}$, and reaches the centre of the gap at a phase $\varphi_n$ of the r-f field. Quantities relating to the synchronous particle are denoted by the subscript 's'. From the design of the machine, the length of the $n^{th}$ gap is given by

$$g_n = \tfrac{1}{4} \beta_{s,n-1} \lambda . \qquad \ldots\ldots (3)$$

The gain in momentum experienced by the proton crossing the gap is then

$$M(\Delta v)_n = e \int_{t_1}^{t_2} E_{z,n} \, dt , \qquad \ldots\ldots (4)$$

with $t_1$ and $t_2$ the times of entering and leaving the gap, respectively.

Assuming that the relative change in velocity across a single gap is small, we make a first approximation that the velocity remains at the value $v_{n-1}$ within the gap. Inserting this on the right hand side of (4), we write $dt = dz/v_{n-1}$, to obtain

$$M(\Delta v)_n = e \int_{-g_n/2}^{+g_n/2} E_0 . \cos(k_{n-1} z - \varphi_n) . \frac{1}{v_{n-1}} . dz$$

which becomes,

$$M(\Delta v)_n = \frac{e E_0}{v_{n-1}} \cos \varphi_n . g_n . \frac{\sin(k_{n-1} g_n/2)}{(k_{n-1} g_n/2)} \qquad \ldots . (5)$$

The last factor on the right is the well known "transit-time correction". It takes account of the fact that particles arriving at the centre of a gap at the stable phase, but with different velocities, will receive different velocity increments. Making use of (3) and inserting $k_{n-1} = 2\pi/\beta_{n-1} \lambda$, we finally obtain

$$(\Delta \beta)_n = \frac{1}{\pi} . \mathcal{E} . \sin\left(\frac{\pi}{4} \frac{\beta_{s,n-1}}{\beta_{n-1}}\right) \cos \varphi_n \quad . . . . (6)$$

with

$$\mathcal{E} = \frac{E_o\lambda}{Mc^2/e} \quad . . . . . . (7)$$

Together with the equations

$$\beta_n = \beta_{n-1} + (\Delta \beta)_n , \quad \text{and} \quad . . . . . . (8)$$

$$\varphi_n = \varphi_{n-1} + 2\pi(\beta_{n-1} - \beta_{s,n-1})/\beta_{n-1} , \quad . . . . (9)$$

equation (6) determines the phase oscillations. Due to our neglect of the radial dependence of $E_z$, the phase motion can be computed independently of the radial motion.

If we consider the synchronous proton, equations (6) and (8) give

$$(\Delta \beta)_s = \frac{1}{\pi} \mathcal{E} \sin\frac{\pi}{4} \cos\varphi_s \quad . . . . . . (10)$$

$$\beta_{s,n} = \beta_{s,0} + n(\Delta \beta)_s \quad . . . . . . (11)$$

That is, the synchronous particle receives the same velocity increment at each gap.

Making use of (2), the gain in radial momentum at the $n^{th}$ gap is given by,

$$M(\Delta \dot{r})_n = -\tfrac{1}{2} r_n e \int_{t_1}^{t_2} \frac{dE_z}{dz} dt$$

$$= -\tfrac{1}{2} r_n \frac{e}{v_{n-1}} \int_{-g_n/2}^{+g_n/2} \frac{dE_z}{dz} . dz , \quad . . . . (12)$$

again assuming that the axial velocity does not change appreciably across a gap. Since the field $E_z$ is non-uniform only at the entrace to the gap, (12) is a point function, to be evaluated at $z = -g_n/2$. Then,

$$\frac{(\Delta \dot{r})_n}{c} = -\tfrac{1}{2}\left(\frac{r_n}{\lambda}\right) . \frac{1}{\beta_{n-1}} . \mathcal{E} . \cos\left(\varphi_n + \frac{\pi}{4} . \frac{\beta_{sn}}{\beta_n}\right) \ldots (13)$$

together with

$$\left(\frac{r_n}{\lambda}\right) = \left(\frac{r_{n-1}}{\lambda}\right) + \left(\frac{\dot{r}_{n-1}}{c}\right) \cdot \frac{\beta_{s,n-1}}{\beta_{n-1}} \quad \ldots \quad (14)$$

and

$$\left(\frac{\dot{r}_n}{c}\right) = \left(\frac{\dot{r}_{n-1}}{c}\right) + \frac{(\Delta \dot{r})_n}{c} \quad \ldots \ldots \quad (15)$$

serves to determine the radial motion.

## 4. RESULTS

In the calculations, the stable phase position was taken to be 30° in front of the peak of the r.f. field. The rate of acceleration was chosen to be 1.640 MeV/m, so that

$$\varphi_s = 30^\circ$$

$$\frac{1}{\pi} E_0 \cdot \sin\frac{\pi}{4} \cdot \cos\frac{\pi}{6} = 1.640$$

Protons injected at an energy of 0.5 MeV ($\beta_0 = 0.0326$) are accelerated through 43 gaps to an energy of 10.13 MeV.

Using these data, the phase motion of particles injected at phases of 70°, 60°, 45°, 30°, 0°, −15°, −25°, −30° has been computed, and the resulting curves are shown in Fig. 1. The oscillations are damped for initial phase values within the range −30° to almost 70°. The −30° particle is in a state of unstable equilibrium, and the 70° particle is only just lost. Phase damping is more rapid at the beginning of the machine and falls off as the energy increases.

Corresponding to each initial phase value, it can be shown that there are two independent pairs of solutions of the equations of radial motion, and from them any other solution can be obtained by linear combination. These solutions are denoted by

(i) $r_1(n)$ and $\dot{r}_1(n)$, referring to a proton injected on the axis ($r_0 = 0$), with some initial divergence $\dot{r}_0$.

(ii) $r_2(n)$ and $\dot{r}_2(n)$, referring to a proton injected at some radius $r_0$, parallel to the axis ($\dot{r}_0 = 0$).

Then some other solutions $r_3(n)$ and $\dot{r}_3(n)$ will be given by the linear combinations

$$\left.\begin{aligned} r_3(n) &= A\, r_1(n) + B\, r_2(n) \\ \dot{r}_3(n) &= A\, \dot{r}_1(n) + B\, \dot{r}_2(n) \end{aligned}\right\} \quad \ldots \ldots \quad (16)$$

For each of the initial phase values, the radial solutions $r_1(n)$, $\dot{r}_1(n)$, $r_2(n)$ and $\dot{r}_2(n)$ have been calculated. The computations were done on the

A.E.R.E. electronic computor. By averaging the velocity increment gained across a gap over a complete cycle of the r-f field, equations (6) and (13) can be converted into two coupled differential equations which in general must be solved numerically. However, the case of the synchronous particle can be treated analytically, and this was done to provide a check. The results were identical with those given by the machine computation.

As a useful and convenient method of presenting the results, the following procedure was adopted. As a criterion that any proton should be accepted by the accelerator, it was stipulated that nowhere in the 10 MeV section should it make a radial excursion further than 0.5 cm. from the axis. (This figure represents half a drift-tube radius.) Then, if a proton is to reach a maximum radius of 0.5 cm at the $p^{th}$ gap, equations (16) give

$$\left.\begin{aligned} 0.5 &= A\, r_1(p) + B\, r_2(p) \\ 0 &= A\, \dot{r}_1(p) + B\, \dot{r}_2(p) \end{aligned}\right\}$$

Hence values of A and B for this particle can be found, and by inserting them in (16) we can obtain $r_o$, $\dot{r}_o$ and $r_f$, $\dot{r}_f$, where the subscript 'f' refers to the protons at 10 MeV.

Using the orbits predicted by the electronic computor, this procedure has been carried out for successive gaps, and $\dot{r}_o$, $\dot{r}_f$ have been converted into angle of divergence (degrees).

The resulting values of $(r_o, \theta_o)$ have been plotted on "phase diagrams", shown in Fig. 2. As the maximum of the radial oscillations is made to move out along the accelerator, corresponding points on the diagram describe a spiral. Since the position of a maximum depends only on the ratio $r_o/\dot{r}_o$, a line drawn through the origin, meeting the spiral in two points, shows that the particle concerned has had two radial maxima within the 10 MeV section, the one closer to the origin furnishing the stricter criterion of acceptance. Since the accelerator is radially symmetrical, a proton represented by $(r_o, -\dot{r}_o)$ must be the same as one denoted by $(-r_o, \dot{r}_o)$, so that the diagrams possess diagonal symmetry. For this reason we get another set of spirals which are diagonal images of the first set, and for each initial phase the pair of spirals leads to a closed area in the diagram, representing the limits of injection radius and divergence within which a proton is acceptable for acceleration.

As can be seen from Fig. 2, synchronous protons can be accepted from a beam of 0.4 cm. radius and ±1.0° divergence, but the diagrams contract and become tilted as we depart from the 30° case. The beam which has been specified for injection into the accelerator has a spot radius of 0.25 cm. and $\pm \frac{1}{2}^o$ divergence, so that it would seem likely that most of the protons injected at phases between 15° and 45° will be accepted. Many others will get through, but until the composition of the actual beam is known, no estimate of the fraction trapped can be made. However, if protons are injected uniformly over the 360° cycle, at least one tenth of them will be accelerated, against the one quarter which would be suggested by considerations of phase trapping alone.

In Fig. 3, the accelerated beams at 10 MeV have been plotted. It will be seen that there has been very considerable damping in divergence, whereas the radial displacement has increased. Thus, synchronous particles will emerge at radii between 0 and 0.5 cms. and with divergences between ±0.2°. In fact, none of the accepted protons will have a divergence much greater than this value.

5. APPROXIMATIONS INVOLVED.

In the above analysis, several different approximations have been made. The most important of these are:

(i) Neglect of the radial dependence of $E_z$. If the field equations are solved for a periodic structure consisting of drift tubes without grid, it is found that the axial field contains a radial term given by $I_0(kr) = J_0(ikr)$, which is important in the first few gaps. The grids will have the effect of reducing this variation, and since protons will not have reached a large radius within the first ten gaps, it should be a good approximation to neglect this term.

(ii) Neglect of penetration of the fields into the drift-tubes. The fields will penetrate into the drift-tubes to some extent, the effect being most important at the beginning of the section where gap and drift-tube lengths are small. The radial impulses received will not, in practice, by the "delta-function" quantities we have employed. Some estimate might be made of the extent of this penetration, but it is difficult to deal with quantitatively.

(iii) Non-uniformity of the axial field at the gap exits could lead to errors. The lines of force of the field must end on a grid surface, and so will not everywhere be parallel to the axis. This effect should be of small importane; again it is not readily susceptible to quantitative investigation.

(iv) Neglect of the magnetic field $H_\theta$. This is a good approximation since $H_\theta$ is proportional to $\beta . E_z$. The focussing force due to $H_\theta$ will then be of order $\beta^2$ times the focussing due to $E_r$. At 0.5 MeV this represents a factor 0.001, and at 10 MeV, 0.02. It is comparable with the effect of relativistic mass increase, and both can safely be neglected here.

(v) The assumption that the relative velocity change across a gap is small, is not a good approximation at the beginning of the accelerator. At the first gap, the relative velocity change is of order 0.1, at the tenth gap it is 0.05, at the twentieth 0.03, and at the fortieth 0.02.

Thus, the approximations involved in the above theory are serious at the first few gaps, but improve after the first ten. The most useful advance would seem to be a theory to take account of the velocity change within a gap, and the radial dependence of the axial electric field. Such a theory could be used in conjunction with the existing drift-tube geometry, which has now been fixed, and some estimate of the best way the fields in each gap can be adjusted for optimum conditions could be obtained. (This adjustment will be necessary when the 10 MeV section is completed, and it should be advantageous to predict the extent of the changes required). Later, some allowance might also be made for penetration of fields into drift tubes and the effects of this investigated.

Such improvements in the theory doubtless will lead to considerable corrections to the phase and radial orbits of individual protons, but may not have any large-scale influence upon the acceptance tolerances predicted here.

## 6. ACKNOWLEDGEMENTS

The author wishes to thank Mr. W. Walkinshaw who directed this work, and Mr. E. J. H. Crouch for his assistance in the computational programme.

T/M 107

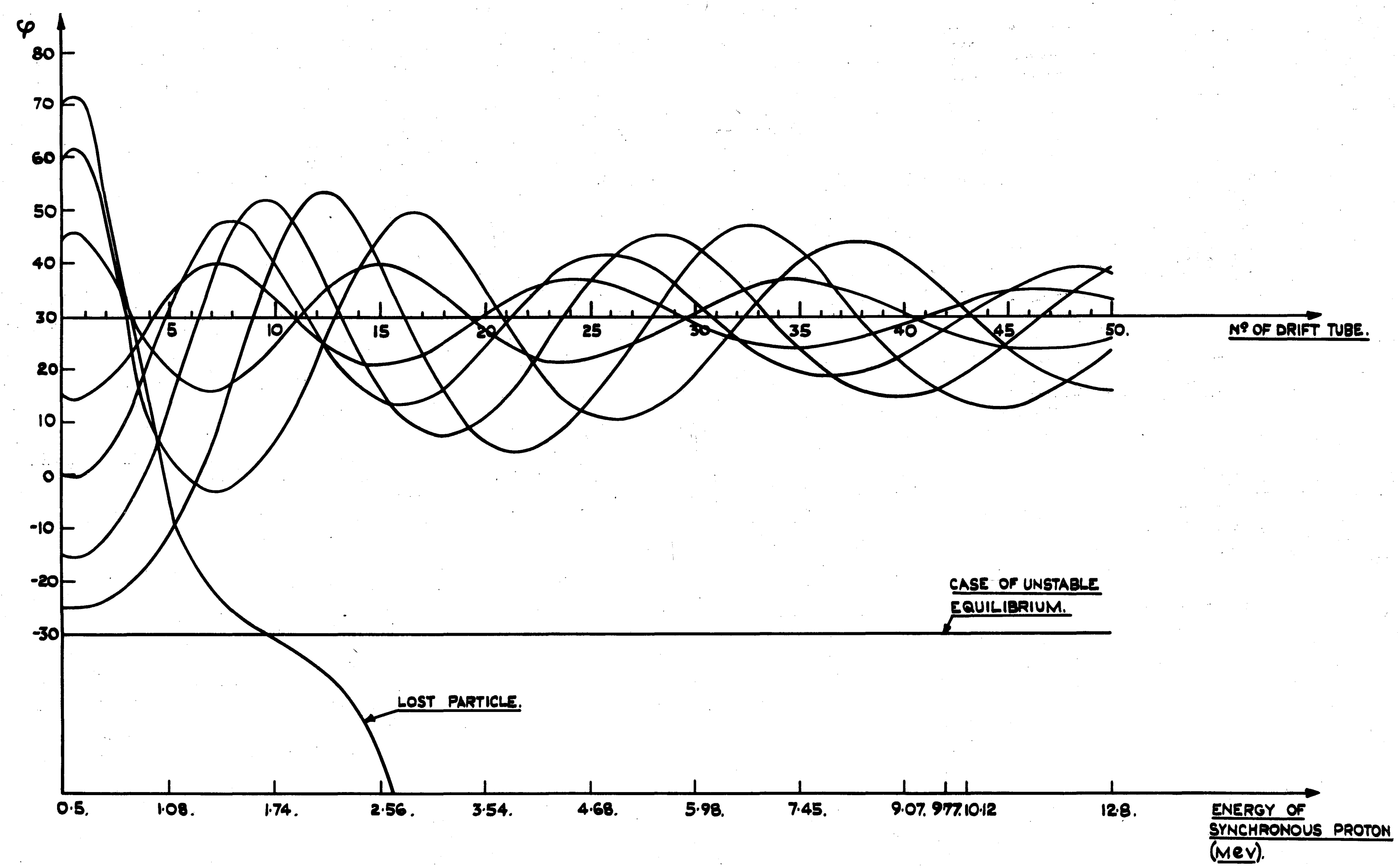


SYNCHRONOUS PHASE = 30°

AER.E. T/M107. FIG. 1. PHASE OSCILLATIONS IN 10 MeV SECTION.

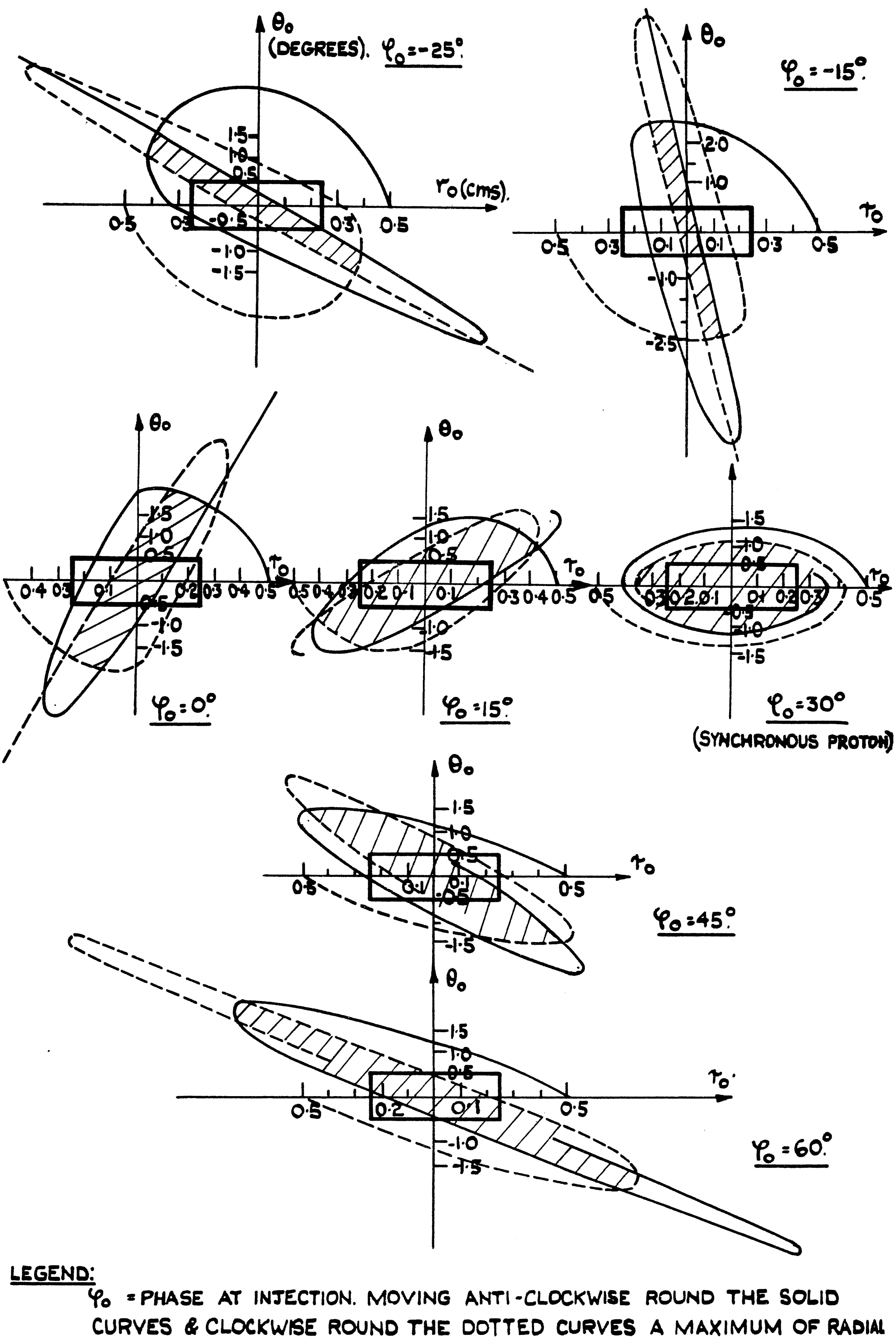


LEGEND:

$\varphi_0$ = PHASE AT INJECTION. MOVING ANTI-CLOCKWISE ROUND THE SOLID CURVES & CLOCKWISE ROUND THE DOTTED CURVES A MAXIMUM OF RADIAL ORBIT MOVES OUT ALONG THE MACHINE.

$r_0$ = RADIAL DISPLACEMENT AT INJECTION.

$\theta_0$ = ANGLE OF TRAJECTORY WITH AXIS AT INJECTION ("DIVERGENCE").

SHADED AREAS REPRESENT RANGES OF INITIAL DISPLACEMENT & DIVERGENCE OF PROTONS ACCEPTED FOR ACCELERATION.

RECTANGLE REPRESENTS BEAM SPECIFIED FOR INJECTION.

A.E.R.E. T/M107. FIG. 2. INJECTION TOLERANCES.

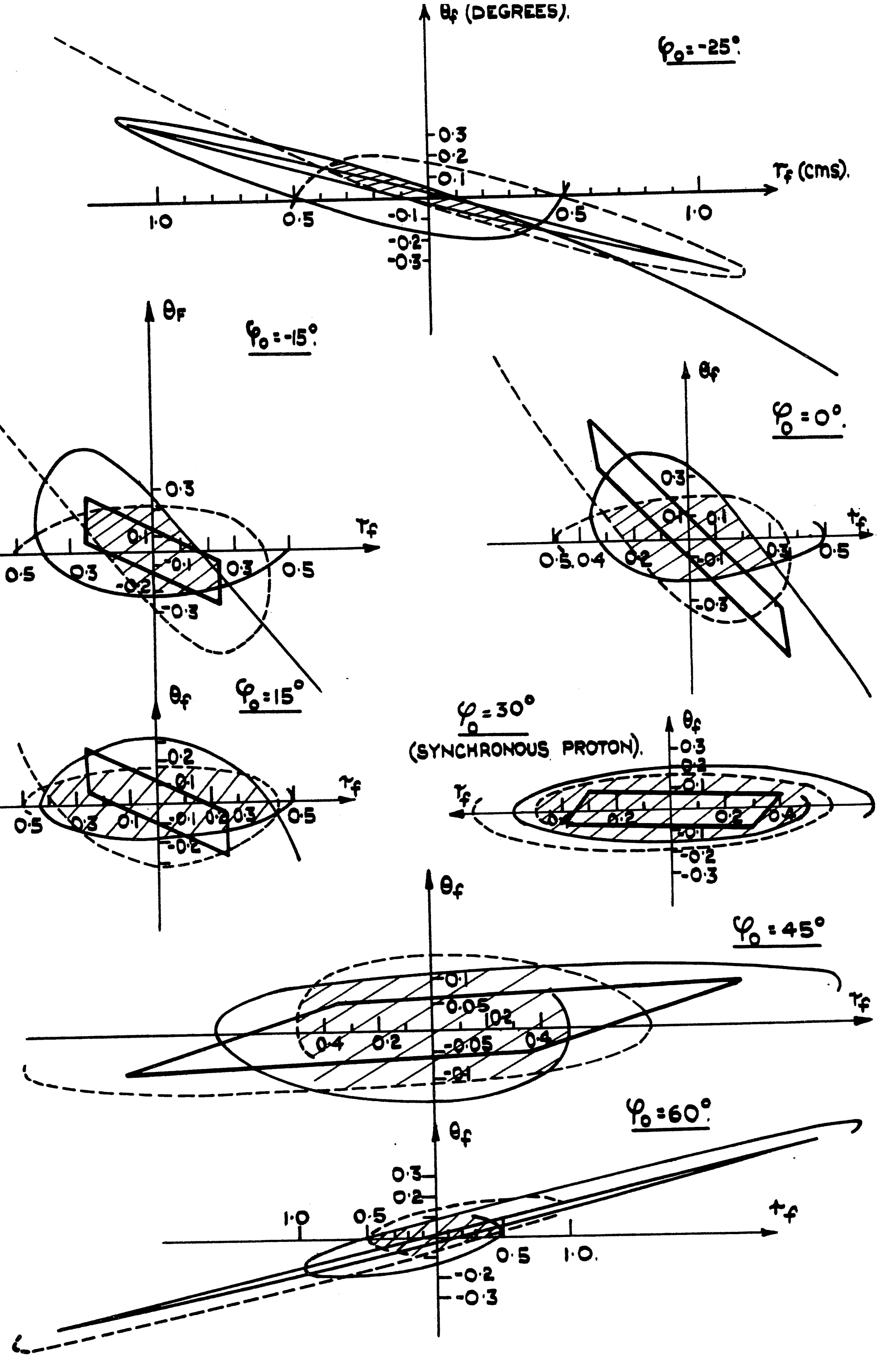


LEGEND:

$\varphi_0$ = PHASE AT INJECTION.

$\theta_f$ = DIVERGENCE AT OUTPUT. (10 MeV). (NOTE: CHANGE OF SCALE OF θ AXIS FOR $\varphi_0$ = 45°.)

$r_f$ = DISPLACEMENT AT OUTPUT.

SHADED AREAS REPRESENT RANGES OF DISPLACEMENT & DIVERGENCE OF OUTCOMING PROTONS WHICH HAVE TRAVERSED THE 10 MeV SECTION WITHOUT MAKING RADIAL EXCURSIONS GREATER THAN 0·5 cm FROM THE AXIS.

PARALLELOGRAMS REPRESENT OUTPUT OF BEAM SPECIFIED FOR INJECTION. (RECTANGLES OF FIG. 2).

A.E.R.E. T/M107 . FIG. 3. OUTPUT BEAM AT 10 MeV.